IOP Publishing Journal of Physics: Condensed Matter
J. Phys.: Condens. Matter **28** (2016) 125001 (9pp) doi:10.1088/0953-8984/28/12/125001

# Tricritical wetting in the two-dimensional Ising magnet due to the presence of localized non-magnetic impurities

**Marta L Trobo[1,2] and Ezequiel V Albano[1,3]**

[1] Instituto de Física de Líquidos y Sistemas Biológicos (IFLYSIB), CCT-CONICET La Plata, UNLP, Calle 59 Nro. 789, (1900) La Plata, Argentina
[2] Departamento de Ciencias Básicas, Facultad de Ingeniería, Universidad Nacional de La Plata, B1900AWN La Plata, Buenos Aires, Argentina
[3] Departamento de Física, Facultad de Ciencias Exactas, Universidad Nacional de La Plata, B1900AWN La Plata, Buenos Aires, Argentina

E-mail: ezequielalb@yahoo.com.ar

Received 27 August 2015, revised 28 January 2016
Accepted for publication 29 January 2016
Published 24 February 2016


**Abstract**

Fixed vacancies (non-magnetic impurities) are placed along the centre of Ising strips in order to study the wetting behaviour in this confined system, by means of numerical simulations analysed with the aid of finite size scaling and thermodynamic integration methods.
By considering strips of size $L \times M$ ($L \ll M$) where short-range competitive surface fields ($H_s$) act along the $M$-direction, we observe localization–delocalization transitions of the interface between magnetic domains of different orientation (driven by the corresponding surface fields), which are the precursors of the wetting transitions that occur in the thermodynamic limit. By placing vacancies or equivalently non-magnetic impurities along the centre of the sample, we found that for low vacancy densities the wetting transitions are of second order, while by increasing the concentration of vacancies the transitions become of first order. Second- and first-order lines meet in tricritical wetting points ($H_{sw}^{tric}, T_w^{tric}$), where $H_{sw}^{tric}$ and $T_w^{tric}$ are the magnitude of the surface field and the temperature, respectively. In the phase diagram, tricritical points shift from the high temperature and weak surface field regime at large vacancy densities to the $T \to 0$, $H_{sw}^{tric} \to 1$ limit for low vacancy densities. By comparing the locations of the tricritical points with those corresponding to the case of mobile impurities, we conclude that in order to observe similar effects, in the latter the required density of impurities is much smaller (e.g. by a factor 3–5). Furthermore, a proper density of non magnetic impurities placed along the centre of a strip can effectively pin rather flat magnetic interfaces for suitable values of the competing surface fields and temperature.

Keywords: tricritical wetting, interfaces, confined materials

(Some figures may appear in colour only in the online journal)

## 1. Introduction

Wetting phenomena and related physical problems such as capillary condensation, thin film growth, epitaxy, interface roughening, etc, are one of the most studied topics in the field of statistical physics and condensed matter sciences [1–9]. This interest is motivated not only by the theoretical challenges posed by the subject, but also by the wide spectrum of practical applications in areas such as adhesion, lubrication, coating and painting, etc. Within this broad context, the Ising model is known to be a powerful tool for the study of wetting behaviour [10–15]. In fact, a suitable procedure is to consider a two-dimensional Ising ferromagnet confined between two walls where competitive surface fields of magnitude $\pm H_s$

 

act, while the bulk field is zero. Under this physical situation the negative (positive) surface field may stabilize a magnetic domain with negative (positive) magnetization, with a $\pm$ interface running in the direction parallel to the confinement walls. For a given value of $H_s$, and in a low temperature regime, such a interface will be attached to either the $H_s > 0$ or the $H_s < 0$ wall with the same probability. However, by increasing $T$ the interface will start to detach from the wall, becoming fully delocalized at a certain effective 'critical' temperature, which depends on the distance $L$ between confinement walls. By properly taking the thermodynamic limit, this localization–delocalization 'transition' becomes a true wetting transition in the infinite sample that is precisely located at $(H_{sw}, T_w)$. By considering short-range surface fields in $d = 2$ dimensions, the wetting transition is of second order, so that even in finite samples one has a rather rough interface that performs excursions from one wall to the other and *vice versa*. Then, motivated by both the basic point of view and the search of potential applications, e.g. in the field of the development of nano- and micro-storage devices, it is useful to explore approaches capable of stabilizing the interface between oppositely oriented magnetic domains. In order to contribute along that line, the aim of the present work is to study the influence of fixed non-magnetic impurities placed along the centre of a strip (i.e. parallel to both the direction of the confinement walls and the interface) on the wetting behaviour of the $d = 2$ dimensional Ising model with short-range surface fields. Within this context, it has been shown experimentally that interfaces of amorphous magnetic Co–Si films can effectively be stabilized [16, 17] with the aid of patterned holes that act as non-magnetic vacancies and are placed along a line. Also, a phenomenological model for an elastic interface interacting with obstacles provides a framework for understanding the stabilization effect in terms of the influence of vacancies on the surface tension of the interface [18].

Furthermore, in a previous paper we proposed that the presence of non-magnetic impurities along the central line of an Ising strip may induce the occurrence of first-order wetting transitions with rather sharp interfaces. Due to the lack of a theoretical framework, we were unable to fully characterize the wetting critical points, so that study was rather qualitative [19]. Now, the recent development of a finite-size scaling theory for wetting with short-range surface fields [20, 21] provides us with a suitable method for the determination of critical points. On the other hand, by using a thermodynamic integration method [22] we are now able to also accurately locate first-order wetting points. In this way, in the present paper we show that lines of both first- and second-order wetting can be well determined, and at the meeting point of these lines the occurrence of tricritical wetting can also be established. It is worth mentioning that according to the mean-field theory for wetting with short-range interactions with the walls, both first- and second-order wetting may be observed [4, 6, 7, 23–25]. Also, tricritical wetting beyond the mean field theory has been early considered [26], and very recently we have characterized tricritical wetting points in the Blume–Capel model by means of Monte Carlo simulations [22, 27]. It is well known that the Blume–Capel model with three states of spin, namely $s = \pm 1, 0$ [28, 29], exhibits the interfacial adsorption of non-magnetic species ($s = 0$), this phenomena being remarkable for the case of wetting transitions [30, 31]. It is then surprising that this rather large 'enrichment' of non-magnetic impurities at the interface does neither affect the critical nature of the wetting transition in the Blume–Capel model nor causes the stabilization of the interface. So, our proposal addresses a rather different physical scenario than that of previous studies [18, 22, 30, 31]. In fact, here we considered non-magnetic impurities placed at fixed positions that cannot naively be modelled by assuming some screening or weakening effect of the coupling constant, as previously considered in a related context [32–35]. In fact, an interface in a bulk two-dimensional system becomes pinned by a line of weak bonds (away from any wall) and then a depinning or delocalization transition is no longer observed [32–35]. On the other hand, as it is discussed below, wetting behaviour with fixed non-magnetic impurities of constant density markedly differs from the case of mobile impurities with a temperature (and crystal field) dependent density, as reported previously for the Blume–Capel model [22].

In summary, our goal is to study the occurrence of tricritical wetting and the stabilization of magnetic interfaces caused by the presence of fixed non-magnetic impurities, in the confined Ising ferromagnet in $d = 2$ dimensions. The manuscript is organized as follows: In section 2 we describe the model used and the simulation method. section 3 is devoted to the presentation and discussion of the results within the context of existing theories, and our conclusions are stated in section 4.

## 2. The Ising model in a confined geometry with non-magnetic impurities, and details of the simulation method

We consider the Ising model where each lattice site of coordinates $(i, j)$ carries a spin $S_{ij}$ that can take on the values $S_{ij} = \pm 1$. Also, a constant density of fixed non-magnetic impurities (or vacancies) is considered with a spin value $S_{ij} = 0$. Simulations are performed in the square lattice by adopting an $L \times M$ geometry with $1 \leqslant i \leqslant L$ and $1 \leqslant j \leqslant M$, where periodic boundary conditions act in the $j$-direction (where the lattice is $M$ rows long), while free boundary conditions are used in the $i$-direction, where we apply surface fields $H_{s1}$, $H_{sL}$ acting on the first and the last row, respectively. Thus, the Hamiltonian is given by [12–15]

$$\mathcal{H} = -J \sum_{\langle ij, i'j' \rangle} S_{ij} S_{i'j'} - H_{s1} \sum_{i \in \text{row } 1, j} S_{ij} - H_{sL} \sum_{i \in \text{row } L, j} S_{ij}, \qquad (1)$$

where $J > 0$ is the coupling constant between spins placed at nearest-neighbour sites, and the symbol $\langle ij, i'j' \rangle$ indicates that the summation is restricted to nearest-neighbour spins only. Just at the centre of the strip, i.e. for $i = L/2$, we place fixed vacancies or non-magnetic impurities ($S_{ij} = 0$), which are taken equally spaced at a distance $l_v$, so that their linear density is $\delta_v = 1/l_v$ (notice that all distances are reported in units of the lattice constant).

In order to study localization–delocalization 'effective' transitions occurring in finite samples, we adopt the antisymmetric situation $H_{s1} = -H_{sL} < 0$, and then we take the thermodynamic limit ($L \longrightarrow \infty, M \longrightarrow \infty$) in order to observe true wetting transitions [10–12, 20, 21].

We perform Monte Carlo simulations by using the standard Metropolis algorithm, and we measure the time in units of Monte Carlo steps per spin (MCS), i.e. during each MCS all the $L \times M$ spins of the sample have the chance of reversing their orientations (flipping) at least once, on average. Typical runs are performed over $4 \times 10^6$ MCS, discarding the first $1 \times 10^6$ MCS to allow for equilibration.

During the simulations, we evaluate the total average absolute magnetization of the film, $\langle |m| \rangle$, obtained from the magnetization $\langle m \rangle$ per lattice site,

$$\langle m \rangle = \frac{1}{N} \sum_{k=1}^{N} S_k, \tag{2}$$

which involves the summation over the total number of spins ($N = L \times M$) in the sample, and $\langle \rangle$ indicates thermal averages over different configurations obtained after disregarding a suitable number of MCS in order to allow for equilibration, as already mentioned. We also compute the square value of magnetization $\langle m^2 \rangle$, and the fourth-order cumulant, which is given by

$$U = 1 - \frac{\langle m^4 \rangle}{3\langle m^2 \rangle^2}. \tag{3}$$

In the absence of a bulk magnetic field, the two-dimensional Ising model undergoes a second-order transition from the ferromagnetic ordered phase to the paramagnetic disordered one, which takes place at the bulk critical temperature ($T_{cb}$) given by $\exp(2J/k_B T_{cb}) = \sqrt{2} + 1$, with $T_{cb} \simeq 2.27 J/k_B$, where $k_B$ is the Boltzmann constant [36]. In the case treated in this paper, with a uniform distribution of vacancies along the centre of the sample and competitive surface fields, the confined Ising magnet now undergoes two types of phase transitions: on the one hand, the standard bulk transition at $T_{cb}$, and on the other hand, a second type of phase transition (i.e. wetting transitions) that occurs at lower temperatures $T_w(H_{s1}) \leqslant T_{cb}$ for small enough absolute values $|H_{s1}|$ of the surface field. Thus, below $T_w(H_{s1})$ the surface field stabilizes a macroscopically thick layer of negative magnetization near the boundary where $H_{s1} < 0$ acts, separated by an interface from the bulk, where the magnetization is positive. At $T_w(H_{s1})$, a transition occurs where this interface gets delocalized. This localization–delocalization 'transition' is the precursor of a true wetting transition occurring in the thermodynamic limit [10–15, 20, 21]. For the Ising model without non-magnetic impurities, this wetting transition is of second order throughout the regime $0 < |H_{s1}| < J$ [37].

## 3. Results and discussion

Figure 1 shows plots of (a) the average absolute magnetization ($\langle |m| \rangle$), (b) the average square magnetization ($\langle m^2 \rangle$), and (c) the cumulant $\langle U \rangle$ versus the surface magnetic field $H_{s1}/J$, as obtained for $T/T_{cb} = 0.85$ and by taking a density of non-magnetic impurities placed along the centre of the strip given by $\delta_v = 0.0833$. According to a recently proposed finite-size scaling theory for critical wetting with short-range surface fields [20, 21], $\langle |m| \rangle$ can be used as a proper order parameter and it scales as

$$\langle |m| \rangle = \xi_{\parallel}^{-\beta/\nu_{\parallel}} \tilde{m} \left( \frac{L^{\nu_{\parallel}/\nu_{\perp}}}{M}, \frac{M}{\xi_{\parallel}} \right), \tag{4}$$

where $\nu_{\parallel} = 2$ ( $\nu_{\perp} = 1$) is the correlation length exponent in the parallel (perpendicular) direction to the interface between domains of different magnetization. Those correlation lengths diverge at criticality according to

$$\xi_{\parallel} \sim \epsilon^{-\nu_{\parallel}}, \tag{5}$$

with $\epsilon \equiv (T - T_w)$, or equivalently $\epsilon \equiv (H - H_{sw})$, and

$$\xi_{\perp} \sim \epsilon^{-\nu_{\perp}}, \tag{6}$$

respectively. Here, $T_w$ ($H_{sw}$) is the critical temperature (corresponding surface field) at the wetting transition, while in equation (4) $\beta$ is the order parameter critical exponent, and $\tilde{m}$ is a suitable scaling function that does not need to be specified here. The generalized aspect ratio is given by $s = L^{\nu_{\parallel}/\nu_{\perp}}/M$, and all our simulations are performed for the choice $s = L^2/M = 9/8$, which allows for a set of integer solutions of $L$ and $M$, i.e. values such as $(L, M) = (12, 128)$, $(18, 288)$, $(24, 512)$, $(36, 1152)$, and $(48, 2048)$, which are commonly used in our calculations.

Based on the fact that $\nu_{\parallel} = 2$ is the only independent exponent for short-range wetting in $d = 2$ dimensions, and by developing scaling arguments, it has recently been shown that $\beta = 0$ [20, 21]. So, since the prefactor $\xi_{\parallel}^{-\beta/\nu_{\parallel}}$ is constant for $\beta = 0$, Monte Carlo simulation data obtained for samples of different sizes but keeping the generalized aspect ratio constant, i.e. the first argument of the scaling function in equation (4) ($s = 9/8$ in the present work), would show an intersection point given precisely by the wetting critical point where the second argument of the scaling function in equation (4) vanishes. From figure 1(a) for $T_w/T_{cb} = 0.85$, one obtains that the critical surface field is given by $H_{sw} = 0.4040(15)$ and $\langle |m(H_{sw})| \rangle \simeq 0.248$. On the other hand, high-order moments of magnetization that scale as

$$\langle m^{2k} \rangle = \xi_{\parallel}^{-2k\beta/\nu_{\parallel}} \tilde{m}^{2k} \left( \frac{L^{\nu_{\parallel}/\nu_{\perp}}}{M} \frac{M}{\xi_{\parallel}} \right), \tag{7}$$

should exhibit the same behaviour. Accordingly, figure 1(b) shows plots of the second order moment of the parameter that also exhibits an intersection point so that for $T_w/T_{cb} = 0.85$ one has $H_{sw} = 0.4035(20)$ and $\langle m^2(H_{sw}) \rangle = 0.087$ (see figure 1(b)), in excellent agreement with the result obtained previously in figure 1(a).

On the other hand, for the fourth-order cumulant ($U$) given by equation (3), the scaling prefactor is independent of the lattice size, so the intersection point for data corresponding to different lattice sizes, but obtained by keeping $s = 9/8$ constant, is naturally observed at $H_{sw}$, namely for $T_w/T_{cb} = 0.85$,

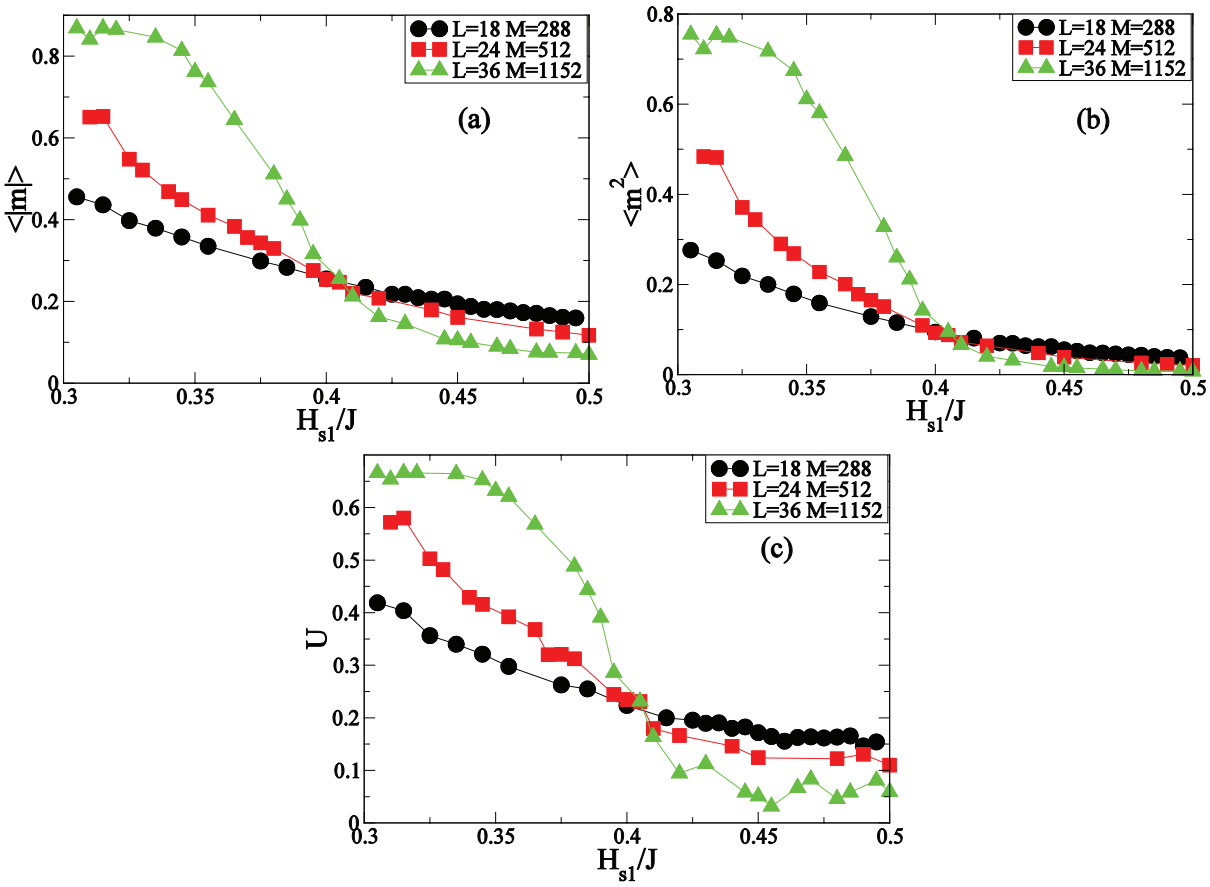


**Figure 1.** Plots of (a) the average absolute magnetization $\langle|m|\rangle$, (b) the average of the square magnetization $\langle m^2\rangle$, and (c) the cumulant $U$ versus the magnitude of the surface field, as obtained for samples of different sizes but keeping the generalized aspect ratio $s = L^2/M = 9/8$ constant, as indicated. Data obtained for $T_w/T_{cb} = 0.85$, for a density of non-magnetic impurities given by $\delta_v = 0.083$. By considering the error bars in the common intersection points of all three measured quantities, the wetting critical filed is located at $H_{sw} = 0.404(3)$. More details in the text.

one has $H_{sw} = 0.4055(20)$, also in agreement with the determinations obtained by measuring both the magnetization and its second moment.

Summing up, by taking into account the error bars of the three common intersection points obtained from $\langle|m|\rangle$, $\langle m^2\rangle$, and $U$, we locate the second-order wetting critical point for $T_w/T_{cb} = 0.85$ at $H_{sw} = 0.404(3)$ for $\delta_v = 0.0833$. This behaviour is typically observed for low density of impurities (not shown here for the sake of space), so the same procedure is performed for different concentrations of non-magnetic impurities in order to obtain second-order critical lines, as is discussed below.

On the other hand, if the density of non-magnetic impurities is properly increased, we start to observe hysteretic effects, as shown in figure 2(a). For this purpose we perform simulations by using two different initial conditions, namely with all spins pointing up, and half of the sample adjacent to the positive (negative) surface field with spins pointing up (down). While for small samples, namely $L = 18$, $M = 288$, hysteresis is no longer observed (see figure 2(a)), by increasing the sample to e.g. $L = 36$, $M = 1152$, hysteretic effects become quite evident (see figure 2(a)). Furthermore, for these large samples the cumulants develop sharp negative peaks (see figure 2(b)). This suggests the occurrence of first-order wetting transitions that cannot accurately be located by using the standard scaling methods discussed above.

In order to overcome this shortcoming, as well as the presence of marked hysteretical effects, we use the thermodynamic integration method that has previously been employed successfully in order to located first-order wetting transitions in $d = 3$ [27] and $d = 2$ [20, 22] dimensions, for a detailed description and discussion of this method see e.g. [38, 39]. In fact, the location of a wetting transition depends on the surface excess free-energy difference $f_s^+ - f_s^-$ between semi-infinite domains in positive (+) and negative (−) spontaneous magnetization, both driven by surface fields, and the interfacial tension between coexisting phases ($f_{int}(T)$), as requested by Young's criterion [3, 4], that is $f_s^+ - f_s^- = f_{int}$. In the case of the Ising model, the interfacial free energy is exactly known since Onsager's exact solution [36], i.e.

$$\sigma = 2J - (\beta^{-1}) \ln\left[1 + \frac{\exp(-2\beta^{-1}/J)}{1 - \exp(-2\beta^{-1}/J)}\right]. \qquad (8)$$

However, by considering non-magnetic impurities along the centre of the sample, as in the present case, an exact solution is not available, so one has to perform a numerical thermodynamic integration. For this purpose one has to use

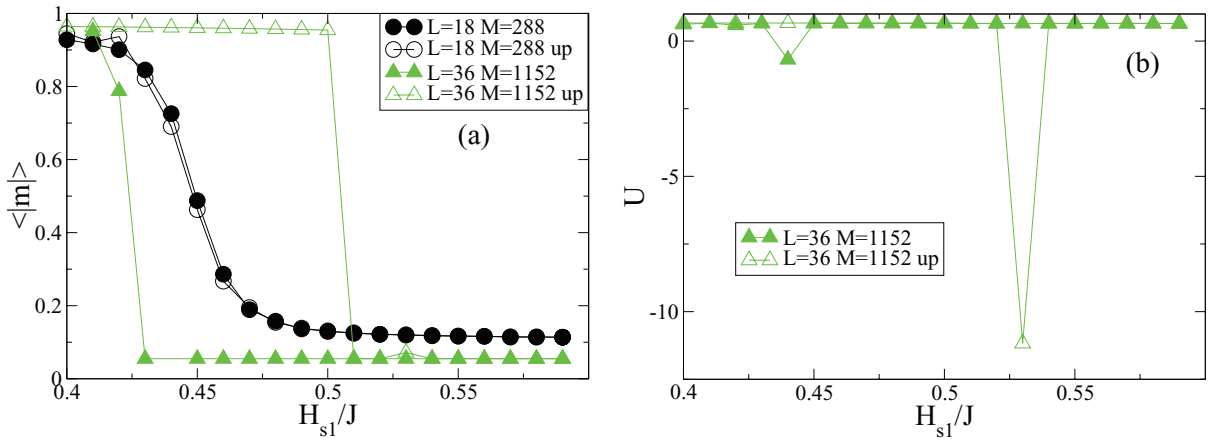


**Figure 2.** Plots of (a) the average value of the absolute magnetization $\langle|m|\rangle$, and (b) the cumulant $U$ versus the magnitude of the surface field, as obtained for $T/T_{cb} = 0.70$ and a density of vacancies given by $\delta = 0.166$. Two types of initial conditions are employed, namely with all spins pointing up (labelled 'up' in the figure), and half of the sample adjacent to the positive (negative) surface field with spins pointing up (down). Notice that in (a) hysteretic effects are negligible for small samples ($L = 18$, $M = 288$), while they become quite large for a bigger lattice ($L = 36$, $M = 1152$). Also, for large lattices the cumulants (b) exhibit negative peaks, as expected for the case of first-order transitions. More details in the text.

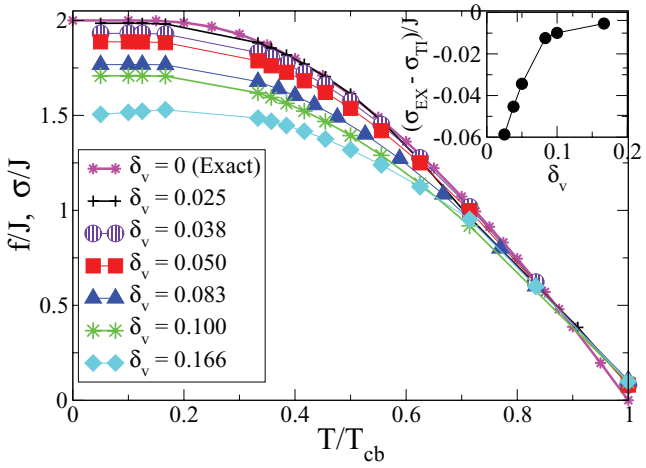


**Figure 3.** Plots of the interfacial free energy ($f$), as obtained by integration according to equation (10), versus $T/T_{cb}$. Results obtained with samples of size $L = 48$, $M = 2048$, and different densities of non-magnetic impurities, as indicated. Data obtained by averaging over $10^7$ MCS after disregarding $2 \times 10^6$ MCS for equilibration. In order to perform the thermodynamic integration (see equation (10)) $T$ is discretized in steps of $\Delta T = 0.05$–$0.01$. The data for $\delta_v = 0$ are taken from the exact solution give by equation (8). The inset shows the dependence on the density of vacancies of the difference between the exact value ($\sigma_{EX}$) as obtained by means of equation (14), and the $T \to 0$ limit ($\sigma_{TI}$) yielded by the thermodynamic integration method. More details in the text.

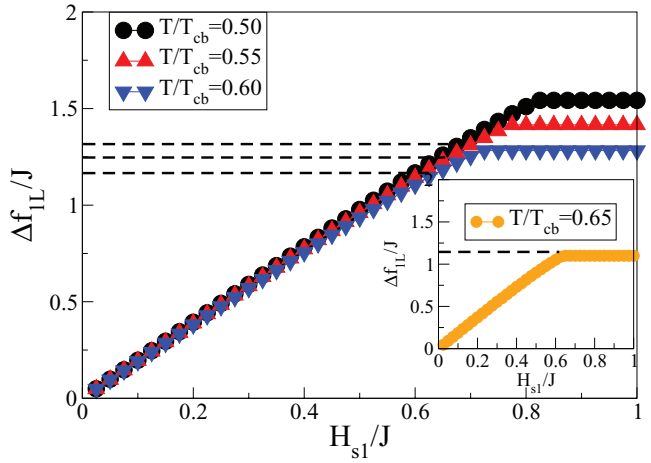


**Figure 4.** Plots of the surface free energy versus the surface field as obtained for different temperatures but keeping the density of non magnetic impurities constant at $\delta_v = 0.30$. The horizontal dashed lines show the interfacial free energies taken from figure 3. The main panel shows clear intersection points of the plotted free energies that allows one to locate first-order wetting transitions. In contrast, for second-order wetting transitions (inset) the accuracy of the determinations by using the thermodynamic integration method becomes limited. Results obtained by using samples of size $L = 48$, $M = 2048$, and averaging over $10^7$ MCS after disregarding $2 \times 10^6$ MCS for equilibration. In order to perform the thermodynamic integration (see equation (13)) the surface field is discretized in steps of $\Delta H_1 = 0.025$. More details in the text.

two reference states: (i) a state with all spins pointing up, and (ii) a state with spins in contact with the wall with $+H_{s1}$ ($-H_{sL}$) pointing up (down), with a flat interface placed along the centre of the strip where fixed non-magnetic impurities are located. Then, by using the relationship between the internal and interfacial energies given by [38, 39]

$$u = (\partial(\beta f)/\partial\beta)_{H,H_{s1},H_{sL}},\ \beta = 1/T, \tag{9}$$

one can perform the following integration:

$$\beta f(\beta) = \beta_0 f(\beta_0) + \int_{\beta_0}^{\beta} u(\beta')\mathrm{d}\beta'. \tag{10}$$

Since in the integration of equation (10) a very large integration interval needs to be avoided, the limit $\beta_0 \to \infty$ can no longer be used. In the present case, one has that $\beta_0 = 20$ (i.e. $T = 0.05$) is already large enough to neglect the entropic contribution. Further details on this method can be found in references [38, 39].

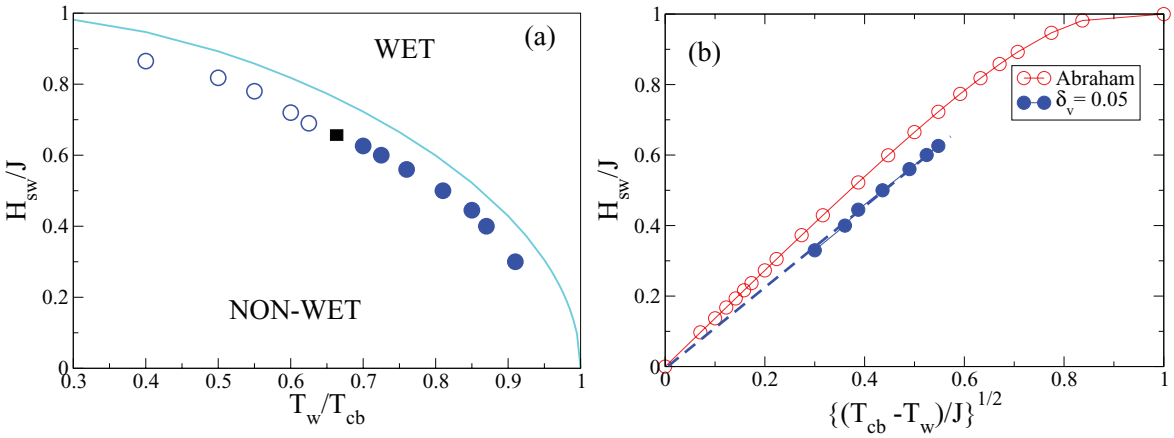


**Figure 5.** (a) Plots of the second-order (solid circles) and first-order (open circles) wetting transition points, in the plane of surface field versus temperature, as obtained for a density of non-magnetic impurities given by $\delta_v = 0.05$. Note that at the meeting point between those curves one has a tricritical wetting transition (solid square) for $H_{\rm sw}^{\rm tric} = 0.65(2)$, $T_{\rm w}^{\rm tric}/T_{\rm cb} = 0.66(2)$. The solid line corresponds to Abraham's exact solution for the pure Ising model in the absence of non-magnetic impurities, taken from reference [37]. (b) Plots of the wetting critical fields ($H_{\rm sw}$) versus $(T_{\rm cb} - T_{\rm w})^{\Delta_1}$ as obtained for Abraham's exact solution (open circles) and numerical data already shown in panel (a) corresponding to $\delta_v = 0.05$ (solid circles). The dashed line has been drawn to guide the eye. More details in the text.

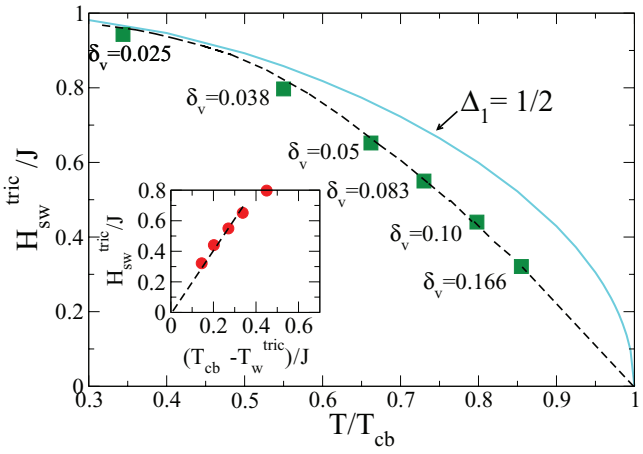


**Figure 6.** Dependence of the tricritical points on the temperature, namely plots of $H_{\rm sw}^{\rm tric}$ versus $T/T_{\rm cb}$ as obtained for different concentrations of non-magnetic impurities, as indicated. The dashed line has been drawn to guide the eye. The solid line corresponds to Abraham's exact solution for the pure Ising model in the absence of non-magnetic impurities, taken from reference [37], which in the limit $T \to T_{\rm cb}$ obeys equation (15) with $\Delta_1 = 1/2$. The inset shows a plot of $H_{\rm sw}^{\rm tric}$ versus $T_{\rm cb} - T_{\rm w}^{\rm tric}$ as obtained by using the data already shown in the main panel. The dashed line has been drawn to guide the eye. More details in the text.

On the other hand, the surface excess free-energy difference ($\Delta f_{1L}$) can be derived by starting from the following relationships:

$$m_1 = -(\partial f_{\rm s}(T, H, H_{\rm s1})/\partial H_{\rm s1})_T, \tag{11}$$

$$m_L = -(\partial f_{\rm s}(T, H, H_{\rm sL})/\partial H_{\rm sL})_T, \tag{12}$$

that link the surface magnetization at the 1st and $L$th walls with the surface free energy and the corresponding surface field. Then, $\Delta f_{1L}$ is just given by

$$\Delta f_{1L} = f_{\rm s}^{(+)}(T, 0, H_{\rm s1}) - f_{\rm s}^{(+)}(T, 0, H_{\rm sL}) = \int_0^{H_{\rm s1}} (m_L - m_1)\mathrm{d}H'_{\rm s1}. \tag{13}$$

Further details on the above (briefly) discussed method have already been published, see e.g. [22]. Then, by using the above-discussed procedure we obtain the dependence of the interfacial free energy $f(\beta)/J$ as a function of the temperature for different densities of non-magnetic impurities (see figure 3). While for $T/T_{\rm cb} \geqslant 0.7$ the interfacial free energy is almost independent of $\delta_v$, at lower temperatures one observes that the presence of non-magnetic impurities causes $f$ to markedly decrease as compared to Onsager's exact solution ($\sigma$) for the pure system.

On the other hand, the interfacial free energy in the presence of fixed non-magnetic impurities can exactly be evaluated in the ground state ($T = 0$). For this purpose let us consider a horizontal strip of width $M$ and height $L$, where a linear density of vacancies given by $\delta_v$ and denoted by a 0 are equally spaced along the central line at $i = L/2$, $(1 \leqslant i \leqslant L)$. So, by placing the $+$ $(-)$ spins in the half-upper (half-lower) part of the strip, the interface looks like

$i = \frac{L}{2}$ .... + + 0 + + + + + 0 + + + + + 0 + + + + + 0 + + + .....

interface .... * * * * * * * * * * * * * * * * * * * * * * * * * * * * * * * * * .....

$i = \frac{L}{2} + 1$ .... − − − − − − − − − − − − − − − − − − − − − − − − − − − − − − − − − −.....,

and the energetic contribution of the $(L/2)$-th line is $\sigma(L/2) = 2J(1 - 2\delta_v)$, while the $(L/2 + 1)$-th line gives $\sigma(L/2 + 1) = 2J(1 - \delta_v)$. Then, the average value gives the interfacial free energy of the ground state, namely

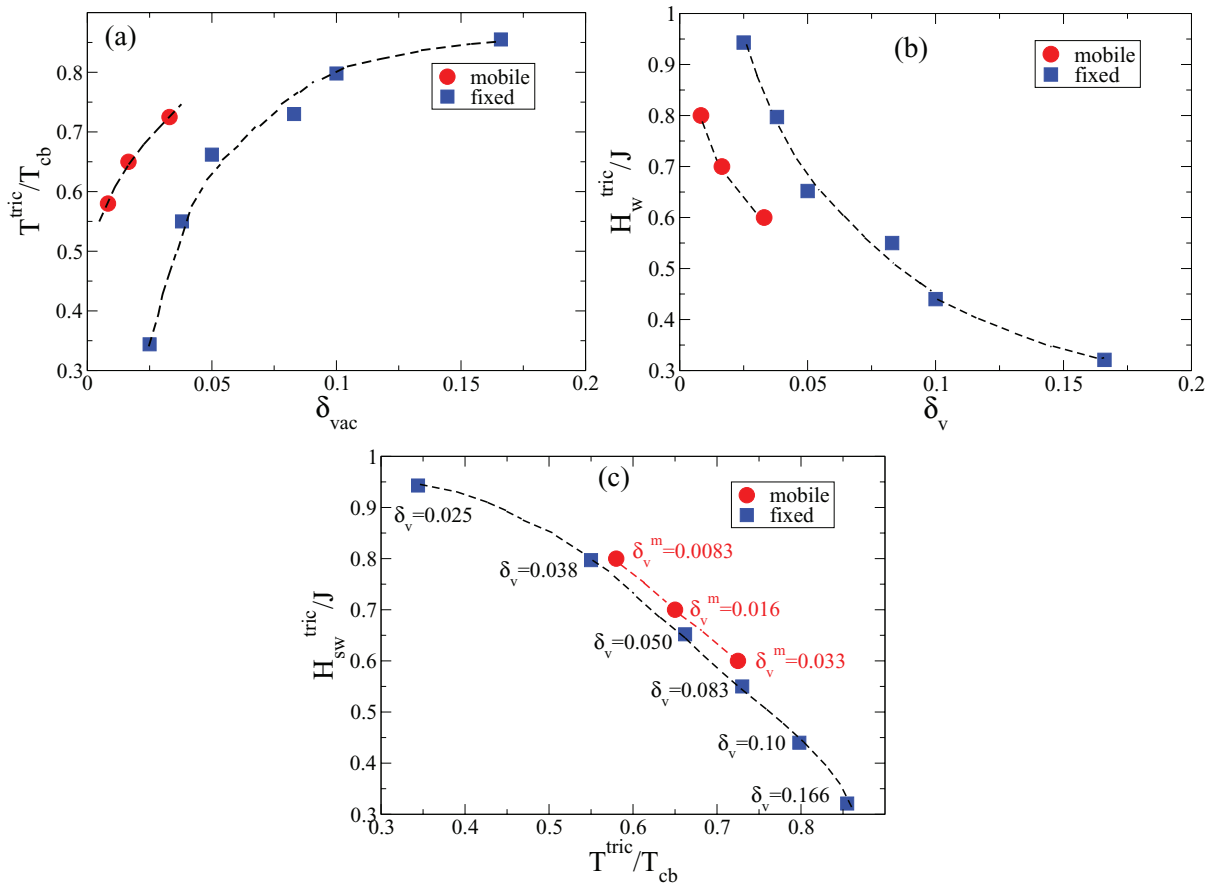


**Figure 7.** (a) Plots of the tricritical temperatures $T^{\rm tric}$ versus the density of non-magnetic impurities. Solid circles (squares) correspond to the case of fixed (mobile) impurities. Data corresponding to mobile impurities are taken from reference [22]. (b) Plots of the tricritical fields ($H_{\rm sw}^{\rm tric}/J$) versus the density of non-magnetic impurities. The symbols are taken as in (a). (c) Plots of the tricritical fields ($H_{\rm sw}^{\rm tric}$) versus the tricritical temperature $T_{\rm w}^{\rm tric}/T_{\rm cb}$ obtained for different densities of non-magnetic impurities, as indicated. In all cases dashed lines are drawn to guide the eye. More details in the text

$$\sigma_{\rm GS} = 2J(1 - \frac{3}{2}\delta_v). \qquad (14)$$

It is worth mentioning that by symmetry the same result is obtained by placing the vacancies in the negative domain, or alternatively by randomly placing vacancies on both sides of the interface (keeping $l_v$ constant). The inset of figure 3 shows a plot of $\Delta\sigma = (\sigma_{EX} - \sigma_{TI})$ versus $\delta_v$ (where $\sigma_{TI}$ corresponds to the extrapolation to $T \to 0$ of the data obtained by means of the thermodynamic integration method, see equation (13)), which indicates that the error in the evaluation of the interfacial free energy is quite small, e.g. $\Delta\sigma < -0.06$. Also, that error decreases monotonically when the density of vacancies increases, while the numerical results always overestimate the exact one.

Furthermore, as discussed above, in order to locate the wetting transition one has to evaluate the dependence of the interfacial free energy at the wall on the surface field as shown in figure 4, namely plots of $\Delta f_{1L}/J$ versus $H_s/J$, as obtained for $\delta_v = 0.30$ and different temperatures. Figure 4 also shows (by means of dashed horizontal lines) the values of the interfacial free energies corresponding to different temperatures taken from the data of figure 3. By equating $f = \Delta f_{1L}$ one can precisely locate first-order wetting transition points resulting in (see figure 4): $H_{\rm sw} = 0.674(5)\,(T/T_{\rm cb} = 0.50)$, $H_{\rm sw} = 0.650(5)\,(T/T_{\rm cb} = 0.55)$, and $H_{\rm sw} = 0.626(5)\,(T/T_{\rm cb} = 0.60)$. However, this method lacks accuracy for a second-order wetting transition (see inset of figure 4) where $\Delta f_{1L}$ saturates for values close to $f$ (at the corresponding temperature of $T/T_{\rm cb} = 0.65$, of course) making it almost impossible to determine the intersection point. However, as discussed above, critical wetting points are accurately determined by using finite-size scaling analysis of the numerical data.

Then, based on the obtained results we can draw phase diagrams of wetting transitions, i.e. plots of the critical points in the plane $H_{\rm sw}$ versus $T_{\rm w}/T_{\rm cb}$, for different values of the concentration of non-magnetic impurities, as e.g. is shown in figure 5(a) for the case $\delta_v = 0.05$. In this case we observe that for a given surface field the wetting critical temperatures tend to decrease, as compared to the case $\delta_v = 0$ that corresponds to the confined Ising ferromagnet whose exact solution has been provided by Abraham [37]. Also, we observe that first- and second-order lines meet in a tricritical point located at $H_{\rm sw}^{\rm tric} = 0.65(2)$, $T_{\rm w}^{\rm tric}/T_{\rm cb} = 0.66(2)$, for $\delta_v = 0.05$.

For a second-order wetting transition, the inverse function $H_{\rm sw}(T)$ of $T_{\rm w}(H_{\rm s})$ behaves as [40]

$$H_{\rm sw}(T) \propto (T_{\rm cb} - T)^{\Delta_1}, \qquad (15)$$

where $\Delta_1$ is the critical exponent that controls the scaling behaviour with the surface field $H_{\rm s}$ near bulk criticality

[41–43]. In $d = 2$, Abraham's exact solution [37] gives $\Delta_1 = 1/2$. So, figure 5(b) shows plots of $H_{sw}$ versus $(T_{cb} - T_w)^{1/2}$, as suggested by equation (15). It is found that Abraham's exact solution obeys the power law with exponent $\Delta_1 = 1/2$ up to $H_{sw} \approx 0.7$, while the solid circles corresponding to second-order wetting transitions with $\delta_v = 0.05$ also obey equation (15), with the same exponent, up to $H_{sw} \approx 0.6$.

We determined the tricritical points for different values of $\delta_v$ by using the above-determined procedure, as shown in figure 6. Since tricritical points lie in the three-parameter space $(H_s, T_w, \delta_v)$, figure 6 can be considered as a projection of the data to the plane determined by $\delta_v = 0$. We found that the tricritical fields tend to increase when $\delta_v$ decreases. The curve becomes almost tangent to Abraham's exact solution close to $T/T_{cb} \approx 0.3$ (see figure 6) and we expect that $H_{sw}^{tric} \to 1$, $T_w^{tric} \to 0$ for $\delta_v = 0$. Regrettably, we are not in condition to further explore the above-mentioned limit by means of numerical simulations, due to the huge computational effort required and the lack of appropriate statistics to achieve reliable results. On the other hand, in the limit $H_{sw}^{tric} \to T_{cb}$ our results depart form Abraham's exact solution, exhibiting almost a linear behaviour. This trend is confirmed in the inset of figure 6, which strongly suggests that equation (15) holds for tricritical points but with $\Delta_1 = 1$. Finally, we would like to compare our results for the wetting behaviour of the confined Ising ferromagnet with fixed impurities placed at the centre of the sample with those previously obtained for the case of mobile vacancies [22]. In the latter, mobile vacancies are naturally considered by using the Blume–Capel model [28, 29] with three spin states, namely $s = \pm 1$ (as in the Ising ferromagnet), and $s = 0$ for the additional state of vacancies. In the Blume–Capel model the density of vacancies is regulated by the crystal field $D$, so the corresponding Hamiltonian reads:

$$\mathcal{H} = -J \sum_{\langle i,j \rangle} S_i S_j + D \sum_{i \in \text{row } 1} S_i^2. \tag{16}$$

It is well known that for $D = -\infty$ the vacancies are expelled and the Blume–Capel model maps the Ising model. So, by taking $D = D^*$ at the centre of the $L \times M$ strip, i.e. for the line $i = L/2$, and $D = -\infty$ otherwise, we allocated mobile vacancies along the centre of the sample [22]. Figure 7 is a set of 3 plots aimed to show the comparison of the influence of fixed versus mobile impurities on the wetting behaviour of the confined ferromagnet. In fact, figures 7(a) and (b) show plots of the tricritical temperature (tricritical field), obtained by keeping the surface field (temperature) fixed, versus the density of vacancies. Also, figure 7(c) shows plots of the tricritical field versus the tricritical temperature, as obtained for different densities of vacancies. We observe a tiny shift of the tricritical points towards the non-wet phase for the case of fixed vacancies, as compared to the case of mobile ones. However, the density of vacancies required to change the wetting behaviour from critical wetting to complete wetting is more sensitive to the presence of mobile than fixed vacancies, e.g. for neighbouring tricritical points one has $\delta_v^{fix} > \delta_v^{mob}$, where the multiplicative factor is close to 3–5.

## 4. Conclusions

We studied the confined Ising ferromagnet in the presence of competitive surface fields and a line of fixed non-magnetic impurities with density $\delta_v$ placed at the centre of the sample, i.e. along the direction of the confinement walls. This type of study is relevant not only for its potential applications, but also from the theoretical point of view. In fact, as early pointed out by Fisher [32]: it is natural to enquire whether an interface in a bulk two-dimensional system can be pinned by a linear imperfection, (away from any wall) and then undergo a depinning or delocalization transition. Within this context we show that such localization–delocalization (wetting) transitions are observed in the presence of a proper density of non-magnetic impurities away from the walls. Furthermore, the observed transitions may be either of first or second order in the limit of high- and low-density of vacancies, respectively. As expected, tricritical wetting points are located at the meeting points between first- and second-order transition lines. So, we show that the physical situation studied here substantially differs from the case where a line of weak bonds is placed away from any wall, so that wetting transitions are no longer expected to occur. Since for low vacancy density one has rough interfaces, characteristic of the critical wetting behaviour, while such interfaces become rather flat for complete wetting in the high vacancy density limit, we also conclude that by choosing a suitable concentration of vacancies it may be possible to regulate the interfacial roughening. We also show that, as expected, the interfacial free energy decreases due to the presence of non-magnetic impurities, and besides our numerical results, we derived the exact solution for the ground state, given by $\sigma_{GS} = 2J(1 - \frac{3}{2}\delta_v)$.

Finally, we conclude that the combination of finite-size scaling and thermodynamical integration methods provides a powerful tool for the study and characterization of physical systems exhibiting both critical and complete wetting behaviour.

## Acknowledgments

We thanks Prof Dr K Binder for helpful discussions. This work was supported by the CONICET and the UNLP (Argentina), UNLP:X11/634; CONICET:PIP 2012/ 0143.

## References

[1] Barabási A-L and Stanley H E 1995 *Fractal Concepts in Surface Growth* (Cambridge: Cambridge University Press)
[2] Kertész J and Vicsek T 1994 *Fractal in Science* ed A Bunde and S Havlin (Berlin: Springer) p 89
[3] Sullivan D E and Telo da Gama M M 1986 *Fluid Interfacial Phenomena* ed C A Croxton (New York: Wiley) p 45
[4] Dietrich S 1988 *Wetting Phenomena* (*Phase Transitions and Critical Phenomena* vol XII) ed C Domb and J L Lebowitz (New York: Academic) p 1
[5] Schick M 1990 *Liquids at Interfaces* ed J Charvolin *et al* (Amsterdam: Elsevier) p 415
[6] Forgacs G, Lipowsky R and Nieuwenhuizen T M 1991 *The Behavior of Interfaces in Ordered and Disordered Systems* (*Phase Transitions and Critical Phenomena* vol XIV) ed C Domb and J L Lebowitz (New York: Academic) p 136

[7] Bonn D and Ross D 2001 *Rep. Prog. Phys* **64** 1085
[8] De Gennes P G, Brochard-Wyart F and Queré D 2003 *Capillarity and Wetting Phenomena: Drops, Bubbles, Pearls, Waves* (Berlin: Springer)
[9] Indekeu J O 2010 *Physica* A **389** 4332
[10] Albano E V, Binder K, Heermann D W and Paul W 1989 *Surf. Sci.* **223** 151
[11] Albano E V, Binder K, Heermann D W and Paul W 1990 *J. Stat. Phys.* **61** 161
[12] Albano E V, Binder K and Paul W 2000 *J. Phys.: Condens. Matter* **12** 2701
[13] Albano E V, De Virgiliis A, Müller M and Binder K 2004 *J. Phys.: Condens. Matter* **16** 3853
[14] De Virgiliis A, Albano E V, Müller M and Binder K 2005 *J. Phys.: Condens. Matter* **17** 4579
[15] Albano E V, De Virgiliis A, Müller M and Binder K 2006 *J. Phys.: Condens. Matter* **18** 2761
[16] Marconi V I 2007 *Phys. Rev. Lett.* **98** 047006
[17] Pérez-Junquera A *et al* 2008 *Phys. Rev. Lett* **100** 037203
[18] Marconi V I, Kolton A B, Capitán J A, Cuesta J A, Pérez-Junquera A, Vélez M, Martín J I and Parrondo J M R 2011 *Phys. Rev.* B **83** 214403
[19] Cotes S M and Albano E V 2011 *Phys. Rev.* E **83** 061105
[20] Albano E V and Binder K 2012 *Phys. Rev.* E **V85** 061601
[21] Albano E V and Binder K 2012 *Phys. Rev. Lett.* **V109** 036101
[22] Trobo M L, Albano E V and Binder K 2014 *Phys. Rev.* E **90** 022406
[23] Binder K, Landau D and Müller M 2003 *J. Stat. Phys.* **110** 1514
[24] Cahn J W 1977 *J. Chem. Phys.* **66** 3667
[25] Schmidt I and Binder K 1987 *Z. Phys.* B **67** 369
[26] Kroll D M, Lipowsky R and Zia R K P 1985 *Phys. Rev.* B **32** 1862
[27] Albano E V and Binder K 2009 *J. Stat Phys.* **135** 991
[28] Blume M 1966 *Phys. Rev.* **141** 517
[29] Capel H W 1966 *Physica* **32** 966
[30] Selke W 1984 *Surf. Sci* **144** 176
[31] Fytas N G and Selke W 2013 *Eur. Phys. J.* B **86** 365
[32] Fisher M 1984 *J. Stat. Phys.* **34** 667
[33] Chui S T and Weeks J D 1981 *Phys. Rev.* B **23** 2438
[34] Burkhardt T W 1981 *J. Phys. A: Math. Gen.* **14** L63
[35] van Leeuwen J M J and Hilhorst H J 1981 *Physica* A **107** 319
[36] Onsager L 1944 *Phys. Rev.* **65** 117
[37] Abraham D B 1980 *Phys. Rev. Lett.* **44** 1165
[38] Landau D P and Binder K 2005 *A Guide to Monte Carlo Simulation in Statistical Physics* 2nd edn (Cambridge: Cambridge University Press)
[39] Binder K 1981 *Z. Phys.* B **45** 61
[40] Nakanishi H and Fisher M E 1982 *Phys. Rev. Lett.* **49** 1565
[41] Binder K and Hohenberg P C 1972 *Phys. Rev.* B **6** 3461
[42] Binder K and Hohenberg P C 1974 *Phys. Rev.* B **9** 2194
[43] Binder K 1983 *Phase Transitions and Critical Phenomena* vol 8, ed C Domb and J L Lebowitz (London: Academic) p 1